Reply to the Comments from Referee #1 for HESS-2018-517

We greatly appreciate the referee for thorough reading of the manuscript and valuable comments, which helped us to improve the manuscript significantly. In the following, we have provided an item-by-item reply to the comments.

Major Comments:

1) Discussion on the required number of gauges: The study provides information on the number of gauges required to estimate areal rainfall within an estimation error (NRMSE) of 20%. Such information would be useful for many purposes including i) the design of new gauge networks, and ii) quantifying estimation errors from the existing networks. However it should be noted that it is BOTH the number and the spatial configuration of the network that determine the estimation error. The interplay between spatial configuration and number of gauges can be easily illustrated using hourly scale results in Figure 5 (bottom-left panel). The authors conclude here that 12 gauges are required at hourly scale for NRMSE to be < 20%. However, from Figure 5, it can be seen that the NRMSE at hourly scale can be brought to within 20% even with 8 gauges, although for a specific spatial configuration. So, from the perspective of gauge network design, meeting the desired error limit with the minimum number of gauges is more useful. On the other hand, with 24 gauges, the NRMSE at hourly scale will be below 20% for all 1000 spatial configurations considered in Figure 5. In short, 20% NRMSE at hourly scale can be achieved with 8-24 gauges depending on their spatial configuration. On average (i.e. not always), 12 gauges ensure <20% NRMSE. I suggest that the authors highlight the role of spatial configuration in section 4 where they provide thumb rules on the number of gauges required at each time scale.

   => Thank you for this suggestion. We agree with the reviewer that "the minimum number of gauges" to reach a certain level of error (NRMSE 20% in our study) will be interesting for certain purposes. Now this point is described in Section 4 along with more analysis to show the role of spatial configuration of the network in estimating areal rainfall uncertainty (Page 6 Lines 23-31). Among the 1,000 combinations for each n-gauge network, we selected "good" and "bad" combinations, 100 cases each, based on the uniformity index defined in Appendix B (it is the uniformity index we used for Fig.6) and calculated their NRMSE. As seen in Fig 5, small errors can be achieved when the gauges are regularly distributed.

2) Consistency in conclusions from Figures 5 and 6: Firstly, if the metric plotted along y-axis of Figure 6 is the ratio of resampled rainfall to true rainfall, then it cannot be negative. Is it defined as (resampled-truth)/truth? The y-axis label and the figure caption should be changed accordingly. While discussing Figure 5, the authors state that "At the daily scale, more than one gauge per 300 km2 would be sufficient to reach the >20% accuracy level. Correspondingly, at the temporal scales of 1-h, 30-min, and 5-min, more than 12, 18, and 33 gauges, respectively, are needed to achieve the same level of accuracy". In lines 15-17 of Page 7, the study concludes that at least 2-5 gauges are required for reliable areal rainfall estimates with "no significant error" and "More than 5 gauges guarantee a high accuracy of areal rainfall estimates". This

conclusion of 2-5 gauges is specific to Figure 6. But the manner in which it is mentioned in Page 7 overrules the conclusions reached via Figure 5 and gives an impression that it is the main conclusion as far as the number of gauges required. The differences between Figure 5 (overall NRMSE for 1000 sub-networks) and Figure 6 (inter-event variability for a particular sub-network) need to be clearly discussed in section 4 and in section 6.

=> We have corrected the Y-axis label and the figure caption (Page 19). Thanks for the correction. As the referee pointed out, we showed the overall estimation error from random possible gauge combinations using Fig.5 and examined the event-based rainfall estimation error from a "well-designed" network using Fig.6. Now this is clearly pointed out in Sect.6 (e.g., Page 8 Lines 28-32 vs Page 8 Line 33- Page 9 Line 3).

3) Effect of spatial scale: Effect of spatial scale: It is expected that the rainfall fields are smoother at coarser spatial and temporal scales. In fact, the behaviour is quantified in the form of correlograms (section 3), where the correlation distance increased with time scale. So, the novelty in the analysis presented in section 5 should be discussed clearly?

=> Section 5 intends to show the uncertainty in final rainfall products due to the selected spatial resolution, no matter how detailed spatial information (from many gauges) was obtained. We aim to quantify how different rainfall events will be considered extreme (Fig.8) depending on spatial and temporal resolution (e.g., extreme rainfall at 5-min scale varies from 54.2 mm to 78.2 mm as resolution increases from 0.1° to 0.01°). In addition, we aim to demonstrate how rainfall data resolution affects frequency and location information of extreme rainfall events (Fig.9) which couldn't be deduced from correlograms (Sect. 3). Please refer to Sect 5 (Page 7) where we made modification.

Specific Comments:

1) Page 3, line 23: Page 3, line 23: The authors mention that the gauges record rainfall every five minutes. As the gauges used are tipping-bucket type, I am assuming that the authors'statement implies that the raw data from the data logger is aggregated every five minutes. Please clarify.

=> yes, that is correct. We have rewritten the sentence as "Raw rain gauge data are aggregated every five minutes"; now Page 3 Line 33.

2) Page 4, line 15: Page 4, line 15: How are zero values treated during log-transformation of the data before estimating correlograms? Furthermore, a discussion on how the readers should interpret the correlograms obtained in the log-transformed space would be useful. For example, the correlation distance of 200 km for the wet season and daily scale is based on the log-transformed data. So, I wonder how this correlation distance in logtransformed data reflects in the non-transformed space (i.e. rainfall values). On the same note, can the authors elaborate why Pearson's correlation is used over Spear-man's correlation? The latter is more robust to non-normality of the data.

=> we used rain value+1 to include zero rainfall; log(0+1)=0. We added more details about how to calculate correlations and the sensitivity of the correlation estimation to log-transformation (from Page 4 Line 31). Interpretation of correlations from transformed data is not straightforward, however, we checked that correlation obtained from logtransformed vs non-logtransformed data yield pretty similar results (please see the figure below).

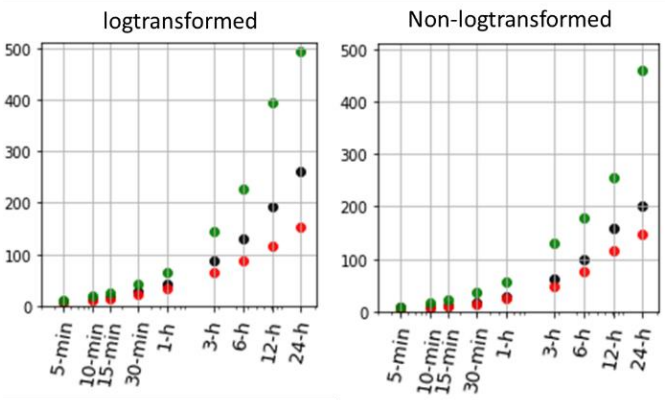

Figure 1 Correlation Distance derived from log-transformed vs non-tranformed data

In addition, we checked the effect of fitting a model to the observed correlation, which was questioned by Referee #2 (comment B4); it turned out that the correlation distance is more sensitive to the fitting model, rather than log-transformation, especially when the spatial scale of the observed correlation is limited to a distance of a few kilometers. This is further discussed in Section 3 (from Page 5 Line 30 & Page 9 25-28).

Please note that Fig.4 is updated. i) RMSE of observed vs fitted correlation is added ii) the model is fitted to correlation values over ranges < 15 km to sample data uniformly in any spatial direction (Page 4 Lines 22-26)

One could use Spearman's correlation, however the Pearson's r is the most commonly used rainfall correlation estimator (e.g., Krajewski et al. 2003; Ciach and Krajewski 2006; Villarini et al., 2008; Peleg et al., 2013; Tokay et al., 2014 and more). To our knowledge, Spearman's correlation is often used to compare rainfall distribution from different sensors (e.g. gauge vs satellite), but barely used to characterize spatial structure of rainfall; meanwhile, Svoboda et al (2015*) used Spearman's and Kendall's correlation in addition to Pearsons'r to compare each other. Due to this reason, we would prefer using Pearson's r for consistency with other studies.*

** all references are listed in the manuscript*

3) Page 6, lines 1-4: All rain rates are wrongly mentioned as mm/day. They should be in mm/h to be consistent with Figure 7. Also, are the percentiles in Figure 7 obtained from the full dataset unlike the analysis in section 4 with 71 events? If so, it should be mentioned at the beginning of the section 5. Moreover, 10% of WEGN records at 30-min scale are lower than 38 mm/h. Please change 40 to 38 in the text.

=> We apologize for the mistake. The unit should be "mm/h" and this is now corrected (Page7 Lines 13-14). Only datasets from the 71 events are used for Section 4 to 5. We added a sentence of "for the heavy rainfall events" at the beginning of Sect. 5 to make it clear (Page 7 Line 10) and also mentioned it in Appendix A (Page 10). We also changed the rain intensity 40 mm/h to 38 mm/h (Page 7 Line 14).

Minor comments:

1) Page 1, line 3: What is "similar approach"? Please add what it is similar to.
   => the sentence is rewritten: "a similar approach, i.e., employing dense gauge networks to catchment-scale areas" (Page 1 Line 3)

2) Page 5, line 15: Consider changing "reach the >20% accuracy" to "reach <20% estimation error".
   => we changed the sentence to "reach <20% estimation error" (Page 6 Line 19)

3) Page 5, Section 5 heading Consider changing "spatial scaling" to "spatial scale" as the former implies spatial scale-invariance.
   => the heading is now "spatial aggregation" (now Page 7)

4) Page 6, line 18: Same as above comment on "spatial scaling"
   => changed to "spatial aggregation" (Page 7 Line 31)

5) Page 8, line 8: It should be "afterward"
   => corrected (Page 10 Line 11)

6) Figure 5: In the box-plot, what does the whisker indicate? Is it [minimum,maximum] or [5th,95th] percentile?
   => the whisker indicates 10^{th}-90^{th} percentiles. The figure caption is updated.

Assessment of spatial uncertainty of heavy ~~local~~ rainfall at catchment scale using a dense gauge network

Sungmin O[1,2,*] and Ulrich Foelsche[1,2,3]

[1]Institute for Geophysics, Astrophysics, and Meteorology/Institute of Physics (IGAM/IP), NAWI Graz, University of Graz, Austria
[2]FWF-DK Climate Change, University of Graz, Austria
[3]Wegener Center for Climate and Global Change (WEGC), University of Graz, Austria
[*]Now at Biogeochemical Integration, Max Planck Institute for Biogeochemistry, Jena, Germany

Correspondence: Sungmin O (sungmin.o@uni-graz.at)

Abstract. Hydrology and remote-sensing communities have made use of dense rain-gauge networks for studying rainfall uncertainty and variability. However, in most regions, these dense networks are only available at sub-pixel scales and over short periods of time. Just a few studies have applied a similar approach, i.e., employing dense gauge networks ~~, to local-scale~~ to catchment-scale areas, which limits the verification of their results in other regions. Using 10-year rainfall measurements from a network of 150 rain gauges, WegenerNet (WEGN), we assess the spatial uncertainty in observed heavy rainfall events. The WEGN network is located in southeastern Austria over an area of 20 $\mathrm{km} \times 15\ \mathrm{km}$ with moderate orography. First, the spatial variability of rainfall in the region was characterised using a correlogram at daily and sub-daily scales. Differences in the spatial structure of rainfall events between ~~wet and dry~~ warm and cold seasons are apparent and we selected heavy rainfall events, the upper 10% of wettest days during the ~~wet~~ warm season, for further analyses because of their high potential for causing hazards. Secondly, we investigated the uncertainty in estimating mean areal rainfall arising from a limited gauge density. The average number of gauges required to obtain areal rainfall with errors less than 20% tends to increase roughly following a power law as the time scale decreases, while the errors can be significantly reduced by establishing regularly distributed gauges. Lastly, the impact of spatial aggregation on extreme rainfall was examined, using gridded rainfall data with horizontal grid spacings from 0.1° to 0.01°. The spatial scale dependence was clearly observed at high intensity thresholds and high temporal resolutions. Quantitative uncertainty information from this study can guide both data users and producers to estimate uncertainty in their own observational datasets, consequently leading to the sensible use of the data in relevant applications. Our findings are generalisable to moderately hilly ~~region in~~ regions at mid-latitudes, however the degree of uncertainty could be affected by regional variations, like rainfall type or topography.

1 Introduction

Rainfall data are one of the most important inputs for hydrological as well as climatological studies and applications. Furthermore, fit-for-purpose information derived from rainfall data is crucial for a wider range of users, such as civil engineers, water resource managers and governments. To meet the needs of diverse user groups, rainfall observational datasets from in-situ

measurement and remote sensing have been greatly enhanced in terms of both data quality and resolution (e.g., Berezowski et al., 2016; Hou et al., 2014; Keller et al., 2015; Yatagai et al., 2012). Often, rainfall data are required as areal estimates at the scale of interest, for instance, at grid or catchment scales. Point measurements from in-situ gauge observations are spatially aggregated or interpolated to estimate the areal distribution of rainfall, and hence the accuracy of areal rainfall data is highly dependent on spatiotemporal variability of rainfall events and density of observation points (Girons Lopez et al., 2015; Hofstra et al., 2010; Villarini et al., 2008; Wood et al., 2000). This limits the understanding of fine-scale rainfall processes, particularly of extreme events (Sillmann et al., 2017). ~~Although relatively higher-resolution~~ Gridded rainfall data from remotely sensed observations are nowadays available at high spatial resolutions (e.g., ~~radar provides rainfall estimates at scales of 1 km/5-min)~~1-5 km^2 for radar data or $0.1^\circ \times 0.1^\circ$ for satellite data). While those data sets are good alternatives to address a number of the issues relating to the scarcity of gauges, ~~still rainfall variability cannot be fully captured at the~~ rainfall variability at sub-pixel ~~scale~~ scales can still not be fully resolved (Peleg et al., 2013; Tokay et al., 2014). In addition, the quality of remotely sensed data strongly relies on gauge-based data that are used for their regional validation and correction ~~(Steiner et al., 1999)~~ (Kann et al., 2015; O et al., 2018b; Steiner et al., 1999).

Addressing the issue of spatial variability and uncertainty of rainfall has been tackled over many years with various purposes. For instance, evaluation of satellite or radar rainfall products involves investigation of ~~small-scale~~ larger-scale rainfall processes to ~~identify the effect of intra-pixel variability of rainfall on the performance of remote sensing~~ assess the ability of remote sensing in capturing the inter-pixel rainfall variability (e.g., Chaudhary et al., 2017; Dhib et al., 2017; Lockhoff et al., 2014) . On the other hand, ~~larger-scale~~ small-scale rainfall processes are of interest to ~~assess the ability of remote sensing in capturing the inter-pixel rainfall variability~~identify the effect of intra-pixel variability of rainfall on the performance of remote sensing(e.g., Ciach and Krajewski, 1999, 2006; Gebremichael and Krajewski, 2004; Habib and Krajewski, 2002; Peleg et al., 2013; Tan et al., 2018; Tokay et al., 2014). To quantify the rainfall uncertainty, observational data from ~~high-resolution~~ highly dense rain-gauge networks have been employed as a ground truth. Peleg et al. (2013) used multiple rain gauges within a radar subpixel area (4 km^2) and examined the contribution of gauge sampling error to the total radar-rainfall estimation error. Using relatively long-term gauge data (5-years), Tokay et al. (2014) analyzed the spatial correlation of rainfall for different seasons and weather systems within the footprint size of microwave satellite ~~sensor~~sensors.

A similar approach employing dense gauge networks can be adopted to diagnose the spatial variability and uncertainty of rainfall at ~~local-scale areas~~ catchment scales (e.g., 100 - 500 km^2). Such ~~a scale is~~ scales are of great interest not only for the evaluation of remotely sensed data, but also for hydrological applications like runoff modelling or gauge network design. Wood et al. (2000) examined the accuracy of areal estimates of rainfall over a 135 km^2 basin according to the HYdrological Radar EXperiment network consisting of 49 rain gauges. The network later provided a six-year rainfall dataset (from 50 gauges) for the study of Villarini et al. (2008), where a comprehensive analysis of temporal and spatial sampling uncertainties was conducted. However, most of the local areas do not have adequately dense gauge networks, which limits the comparison and verification of findings from the aforementioned studies across diverse rainfall regimes.

More recently, Schroeer et al. (2018) employed the WegenerNet Feldbach region (WEGN) and the surrounding operational rain gauge stations to sample summertime convective extreme events at sub-hourly to hourly scales and found a power law

decay of the event maximum area rainfall with increasing interstation distance. In this paper, in order to contribute to the effort for better and more broadly assessing the uncertainty of rainfall at fine scales associated with the spatial variability of ~~local~~ rainfall, we employed 10-year rainfall data from ~~WegenerNet Feldbach region (WEGN)~~the WEGN, a high-density network in southeastern Austria (Kirchengast et al., 2014). The network includes 150 rain gauges deployed over an area of $\simeq$ 300 km^2, approximately corresponding to one gauge per 2 km^2. First, following previous studies (e.g., Villarini et al., 2008; Peleg et al., 2013; Tokay et al., 2014), we quantified the spatial variability of rainfall utilizing a corrologam between the gauges to understand the spatial characteristics of rainfall in the region.

Second, we investigated the uncertainty in estimating areal rainfall ~~based on~~ caused by a limited number of point observations. Given that the properties of individual rainfall events can be different from all-event averages (Ciach and Krajewski, 2006; Eggert et al., 2015), we focused on ~~potentially high-impact events~~ events with a potentially high impact, which we defined as the top 10% wettest days during the ~~wet~~ warm season. The accuracy of areal rainfall estimation is a long-standing issue, e.g., in catchment modelling because error and uncertainty in rainfall data can propagate into large variations in simulated runoff, and thus it has been dealt with in diverse manners. For instance, the influence of spatial representations of rainfall input to runoff errors has been demonstrated through modelling studies (e.g., Bárdossy and Das, 2008; Xu et al., 2013) or the error in catchment-scale areal mean rainfall has been directly quantified by employing high-resolution gauge data (e.g., Wood et al., 2000; Villarini et al., 2008; Ly et al., 2011). We followed the latter approach using the WEGN rainfall data.

Finally, we ~~assessed the impact of spatial averaging on extreme rainfall~~ compare extreme rainfall at different spatial and temporal scales using gridded rainfall fields to quantitatively assess the impact of spatial averaging on the definition of extremes. The identification of rainfall extremes based on intensity thresholds is common practice, however, the considered spatial scale of rainfall data defines different sets of extreme events (Eggert et al., 2015), potentially affecting threshold-based early warning systems (Marra et al., 2017). Although gridded datasets have been used in a range of applications like assessments of climate change impacts or evaluation of climate models, a common caveat of using the datasets in the study of extreme rainfall is that the quality of gridded rainfall data is highly constrained by the location and density of input weather station data (Hofstra et al., 2010; Prein and Gobiet, 2017). By contrast, the quasi-regular configuration of WEGN on an approximately 1.4 km x 1.4 km grid permits robust examination of the frequency and intensity of rainfall extremes at various horizontal resolutions.

Consequently, this study aims to assess spatial uncertainty of ~~local-scale rainfall~~ rainfall at catchment scale using rain gauge data, with a focus on heavy and extreme rainfall events. This paper is structured as follows. Section 2 describes WEGN rain gauge data and regional rainfall climatology. Section 3~~to Sect.~~, Sect. 4, and Sect. 5 present the results of the data analysis. We close with discussion and conclusions in Sect. 6.

2 WEGN rainfall data and regional rainfall climatology

The 10-year rainfall data (2007-2016) are obtained from the WEGN Feldbach region network in southeastern Austria (Kirchengast et al., 2014). Of 154 weather stations, 150 stations that are equipped with tipping-bucket rain gauges are used in this study (Fig. 1). ~~The gauges record rainfall~~ Raw rain gauge data are aggregated every five minutes. Errors in the rainfall data were

comprehensibly analysed and corrected by O et al. (2018a). The gauges are almost uniformly spaced over an area of 20 km × 15 km with moderate topography (about 260 to 520 m asl). The inter-gauge distances range from approximately 0.7 km to 23.4 km. The gridded fields of rainfall are constructed by an inverse distance weighting (IDW) on a 200 m × 200 m Universal Transverse Mercator grid. WEGN station and gridded data products are available at www.wegenernet.org.

Southeastern Austria including the Feldbach region is influenced by both continental and Mediterranean climates. The region receives high amounts of rainfall during summer months. The occurrence of thunderstorms and hail is higher than in other parts of Austria (Matulla et al., 2003). Figure 2 shows average diurnal variations of rainfall and temperature over the entire network during the study period. The WEGN area is characterized by ~~hot~~ warm and wet months from May through September (hereafter "~~wet~~ warm season") and relatively cold months without much rainfall during the remaining seven months (hereafter "~~dry~~ cold season"). The average monthly rainfall is 102.8 mm in the ~~wet~~ warm season, while 48.9 mm in the ~~dry~~ cold season. The diurnal signal is more clearly seen in the ~~wet~~ warm season for both rainfall and temperature. Rainfall maxima occur in the early afternoon through midnight, shortly after maximum temperature, implying that a major contribution to the ~~wet~~ warm season rainfall is from short-duration convective events. Because diurnal heating plays an important role in triggering thermal convection, most inland regions show afternoon rainfall maxima (Dai et al., 2007).

3 Spatial variability of rainfall

The spatial structure of rainfall events is studied using the Pearson's correlation coefficient between all pairs of rain gauges. Pearson's r is the most commonly used rainfall correlation estimator (e.g., Ciach and Krajewski, 2006; Jaffrain and Berne, 2012; Peleg et a . At sub-daily and daily timescales from 5-min to 24-h (06-06 UTC), the correlation of rainfall among rain gauges is calculated for each year. One year period includes a set of ~~wet~~ warm season (May to September) and ~~dry~~ cold season (October to next April). The incomplete years (i.e., first and last years) are excluded from the calculation of all-months (May to next April), whereas the ~~wet and dry~~ warm and cold seasons have 10 annual curves each. ~~Figure 3 shows the spatial correlation of all-months, wet, and dry seasons for four selected accumulation times. Following Villarini et al. (2008), we~~ The correlation values in each period were then sorted according to the separation distance of gauge pairs and averaged into the nearest 1-km distance bins. We fitted a three-parameter exponential function to the ~~observed~~ average correlations. The ~~spatial~~ distance bins for the fitting model were taken up to and including 15 km given the network dimension, which means that rainfall data pairs were sampled uniformly for any spatial direction. The spatial correlation (r) at separation distance h is:

$$r(h) = c_1 \, exp\left[-\left(\frac{h}{c_2}\right)^{c3}\right] \tag{1}$$

where $c1$ ~~is the nugget~~ represents the nugget effect, $c2$ is the correlation distance, and $c3$ is the shape factor. ~~To reduce bias in the Pearson's estimates due to non-normality of rainfall, a logarithmic transformation~~ The parameters are determined by least-squares curve fitting. Figure 3 shows the spatial correlation of all-months, warm, and cold seasons for four selected accumulation times. A logarithmic transformation ($log(x+1)$ to keep zero rainfall) is applied to the data~~(Habib et al., 2001; Jaffrain and Be . The function parameters tend to be sensitive to factors like rainfalltype or sample size and thus we~~ . As the transformation

make rainfall data conform more closely to the normal distribution, the effects of extreme values on correlation coefficients is mitigated (Habib et al., 2001; Jaffrain and Berne, 2012). This results in slightly lower correlations (not shown), however, the overall pattern of correlation decay curves remains unaffected.

Many factors are known to affect the spatial correlation structure in rainfall. For instance, Habib et al. (2001) examined the sensitivity of correlation estimation in rainfall to sample size or extreme rainfall events and Huff and Shipp (1969) demonstrated how the rate of correlation decay varied with different rainfall types. We therefore do not make a direct comparison ~~with other studies in terms of absolute values. Nevertheless, the functions~~ of correlation values with those from other studies, yet we still observe that the behaviors of the correlation decay found in this study ~~show a~~ are in broad agreement with ~~those from previous~~ spatial rainfall correlation structures reported in the aforementioned studies. First, longer accumulation times show higher ~~zero-distance correlation (nugget~~$c1$ (i.e., smaller microscale variations) and longer correlation distance values. Second, short-range correlation decreases rapidly with increasing separation distance, particularly at sub-hourly scales.

The ~~wet~~ warm season shows higher spatial variability of rainfall compared to the ~~dry~~ cold season, due to a higher proportion of convective events. The correlation curves of all-months show a more similar pattern with the ~~wet~~ warm season, as expected, given that most of the rainfall events are concentrated during the ~~wet~~ warm season (see Sect. 2). Tokay et al. (2014) found substantial year-to-year variations especially during autumn and spring. Similarly, WEGN rainfall shows marked interannual variability, but also during the ~~wet~~ warm season. It should be noted that the correlation functions of the ~~dry~~ cold season start with lower ~~nugget~~ $c1$ values than of the ~~wet season. The nugget implies~~ warm season, meaning larger measurement errors and microscale variability of rainfall. Because WEGN does not accurately capture solid precipitation (O et al., 2018a), since only few gauges are heated, systematic errors between neighboring gauges can be greater during the ~~dry~~ cold season, possibly yielding the low ~~nugget~~ $c1$ values.

Figure 4a-c summarizes the time dependence of the three parameters. Synthesized parameters here are obtained from the fitting function that is constructed by averaging yearly correlation values in each distance bin. Nugget effect values range from ~~0.73~~ 0.71 to 0.98 for the ~~dry~~ cold season, while from ~~0.89 to 1.00 for the wet~~ 0.85 to 0.99 for the warm season. The correlation distance of the ~~dry season is stretched up to around 200 at the 6-~~cold season at the 3-h ~~scale, while the same distance is observed~~ is nearly corresponding to the correlation distance at the 24-h scale in the ~~wet~~ warm season. The parameter values of all-months are located between those of ~~wet season and dry~~ warm season and cold season. We found that the ~~general behaviour of nugget~~ dependency of nugget effect and correlation distance on times scale is similar to the results by Villarini et al. (2008). The nugget effect parameter changes sharply at smaller timescales, while the correlation distance appears to be more sensitive for larger timescales. The shape factor of this study, however, does not show a ~~uniform~~ clear increasing or decreasing trend. This is consistent with findings from Peleg et al. (2013) and Tokay et al. (2014). We selected the three-parameter model for the function fitting, because the model shows the minimum root-mean-square error (RMSE) between observed and fitted correlation values across all time scales among the several tested models (Figure 4d). However, we also found that a two-parameter function (i.e., we set shape factor =1) is fitted comparably well and furthermore, correlation distance over large time scales decreases significantly when the two-parameter model is used. However, this model uncertainty does not affect the characteristics of the parameters including their dependence on time scale and their seasonal differences. Nonetheless, when the spatial scale of

observed correlations is limited to a distance of a few kilometers (e.g., accumulation times of >6-h for warm season), the fitted correlation distances should be interpreted with caution. Interested readers may obtain a more detailed discussion of the fitting model in Svoboda et al. (2015).

4 Accuracy of areal rainfall estimation during heavy rainfall events

In this section we investigate data uncertainty associated with areal rainfall estimation. In particular, the study focuses on high-impact rainfall events. While heavy rainfall is one of the major hydrological hazards, its accurate spatial representation over an area remains a subject worthy of inquiry. Based on daily rainfall (≥ 0.2 mm d^{-1}), those days falling in the ~~upper 10th percentile during the wet~~ 90th–100th percentiles during the warm season are defined as heavy rainfall events. As a result, a total of 71 events are selected. The ~~mean~~ median of gauge-averaged accumulations is ~~31.5~~ 28.1 mm d^{-1}, with a range of 19.8 mm d^{-1} to 64.1 mm d^{-1}. General information on the selected events can be found in Table A1.

We assume that the mean areal rainfall of a full density network represents the "truth"~~(see also Villarini et al., 2008)~~. The areal rainfall of n-gauge networks (n = number of gauges) is calculated ~~with 1,000 possible combinations and then~~ and compared with the true rainfall ~~.~~ to quantify the accuracy of areal rainfall estimation with low-density networks (see also Villarini et al., 2008) . Each n-gauge network consists of randomly selected 1,000 possible gauge combinations. The 1-gauge network has 150 cases. As shown in Fig. 5a, the average and spread of normalized ~~root-mean-square errors (NRMSEs)~~ RMSEs of areal rainfall ~~estimated from low-density networks~~ estimation tend to decrease with rising gauge number. The number of gauges required to obtain areal rainfall with NRMSEs lower than 20% is given as a function of time resolution in Fig. 5b. The curve (in black) roughly exhibits power-law behavior; $74.19 \times t^{-0.44}$, where t is the time resolution (minute). At the daily scale, more than one gauge per 300 km^2 would be sufficient to reach ~~the >~~a <20% ~~accuracy level~~estimation error. Correspondingly, at the temporal scales of 1-h, 30-min, and 5-min, on average more than 12, 18, and 33 gauges, respectively, are needed to achieve the same level of accuracy. Villarini et al. (2008) found that four gauges are necessary at the daily scale for the same accuracy level for an area of 135 km^2. Heavy events are not explicitly considered in their study.

One should note that the use of randomly selected gauge combinations only offers a rule of thumb about the required number of gauges to minimize uncertainty in areal rainfall estimates. Additionally, we wanted to see the role of gauge distribution in determining the estimation error. So we selected 'good' and 'bad' distributions, 100 cases, respectively, out of the 1,000 combinations for each n-gauge networks that ranked in the top 10% and bottom 10% based on the area-of-influence (see Appendix B). As seen in Fig 5a (red crosses), the smallest estimation error is obtained with regularly distributed gauges. In other words, a well-designed gauge network allows to meet the desired error limit with a smaller number of gauges (grey curve in Fig 5b). For example, at a 1-h scale, the 20% estimation error can be reached using uniformly distributed 8 gauges, however, the same level of accuracy cannot be guaranteed even with 23 rain gauges if their spatial configuration is not properly structured.

Additionally, the effect of gauge density on event-based rainfall statistics is assessed in Fig. 6. Daily rainfall accumulation and peak hourly rainfall of the 71 heavy daily events are recalculated using predefined sub-networks with gauges ranging

from 1 to 16. The gauges are uniformly spread; the definition of the sub-networks can be found in Appendix ~~A~~B. While the sub-network with only one gauge exhibits large overestimation errors for both total and peak rainfall, employing an additional gauge already significantly reduces the degree of errors and yields underestimation error more frequently than overestimation. Note that Austrian weather service (ZAMG) has two operational stations over the actual WEGN area. Given that convective storms occur on scales of a few kilometers, low-density gauges over the region are likely to miss the core of ~~storms~~storm. On the contrary, low-density gauges ~~often~~ can also overestimate rainfall intensities by capturing only the core of ~~storms~~storm, but the magnitude and frequency of ~~the~~ these errors appear slightly less than those of the underestimation ~~error~~errors. There is no significant difference in either average error or spread of errors from more than 10 gauges, as expected from Fig. 5.

5 Impact of spatial ~~scaling~~ aggregation on extreme rainfall

We next focus on the uncertainty of area- or grid-averaged rainfall relating to ~~data spatial resolution~~spatial data resolution for the heavy rainfall events. Figure 7 compares rainfall percentiles among the gauges. Grey lines mean a 10-90th percentile range of rainfall intensities at a given percentile bin. For example, at the 30-min scale, the 99.9th percentile (the top 0.1%) rainfall intensity corresponds to roughly 45 $\mathrm{mm\,h^{-1}}$ at most gauges, while it exceeds 52 $\mathrm{mm\,h^{-1}}$ at certain gauges. It is also seen that 10% of WEGN gauges (i.e., 15 gauges) records are found to be lower than ~~40~~ 38 $\mathrm{mm\,h^{-1}}$. The upper tail of rainfall distribution shows strong spatial variation. Such point-scale extreme rainfall features will be completely missed unless there exist dense rainfall observations, or they are inherently smoothed out in gridded data.

In fact, many studies have pointed out that the use of gridded rainfall data can lead to erroneous analyses of small-scale extremes because of the limited number of point observations ~~(Hofstra et al., 2010; Tozer et al., 2012; Contractor et al., 2015; Prein and Gobi~~ (Contractor et al., 2015; Hofstra et al., 2010; Prein and Gobiet, 2017; Tozer et al., 2012). In addition to the high-resolution, the regular distribution of WEGN gauges enables generating gridded rainfall fields that are homogeneous in space, and, consequently, robustly assessing uncertainty in rare and extreme rainfall represented in the data.

We generated gridded data ~~at~~ using all 150 WEGN gauges and rescaled the data into horizontal resolutions from 0.01 to 0.1 degree (hereafter HR01 to HR10). Spatial aggregation begins from the top-left corner towards the bottom right and the remaining southern and/or eastern part of the grid is discarded (see Fig 9). HR01 corresponds to about 1.1 km and 0.8 km in latitudinal and longitudinal directions, respectively. Figure 8 shows the 99.9th and 99th percentiles of heavy rainfall intensities as a function of space-time scales. ~~HR01 clearly portrays the benefit of using dense networks to capture fine-scale extreme values, however spatial aggregation brings about the smoothing of rainfall intensities, notably~~ Although temporal aggregation more significantly alters the definition of extremes, the impact of spatial aggregation is also notable, particularly at the sub-hourly scales. The ~~decrease in~~ 5-min ~~rainfall intensity~~ extreme intensity deceases from HR01 to HR10 ~~is~~ by 30% for the 99.9th percentile while it ~~is~~ decreases by 20% for the 99th percentile.

Meanwhile, ~~the spatial scaling~~ although the spatial aggregation impact is much less pronounced at a daily scale, ~~where~~ the selected spatial scale still affects statistics of extreme areal rainfall, such as daily extreme frequency. This is shown in Fig. 9, which illustrates the occurrence of days above a selected threshold; top 5% of heavy rainfall events at HR01. The concept

of the exceedance probability above thresholds is widely used in analyses of rainfall-triggered risk. ~~Several HR01 sites have experienced~~ Some HR01-scale sites appear to experience extreme rainfall more frequently than ~~others~~other part of the region. In other words, high-resolution data well-represent spatial variation and frequency of rainfall extremes, neither of which is seen in lower-resolution data. Many existing gridded datasets are not likely to fully sample such site-level extreme events owing to ~~their spatial scales being limited by sparse observation used to produce the dataset~~limited spatial resolution. The exceedance probability of extreme rainfall across spatial resolutions is given in Fig. 10. The impact of different data resolutions on extreme rainfall occurrence is pronounced in ~~the~~ both lower and upper tails. The 10-year rainfall maximum appears to be 68.4 mm/day at HR10, but 104.4 mm/day at HR01~~. Over the~~ ; the maximum record over the entire WEGN area ~~, the maximum record~~ is 64.1 mm/day~~; +7% to +63% of increases in extreme rainfall intensities are observed~~ , so the ratio of the site-to-areal extreme rainfall ranges from 1.07 to 1.63 depending on the considered spatial scale.

6 Discussion and conclusions

The understanding of spatial uncertainty in ~~local~~ heavy rainfall at fine scales has been hampered by the limited availability of suitable and reliable observational datasets. Although high-resolution radar data are often used to study small-scale rainfall variability, the use of the radar data is dubious, as indicated by Svensson and Jones (2010), owing to their indirect measurements of rain and relatively short records. In this study, we used the 10-year rainfall measurement data from the 150 rain gauges, uniformly spaced over the WEGN network in southeastern Austria. First, to quantify rainfall variability, spatial correlation between the gauge records ~~is~~ was examined. We found that the degree of ~~rainfall spatial~~ spatial rainfall variability can be substantially different not only within years (~~wet versus dry~~ warm versus cold seasons) but also between years. This implies that long-term data should be considered ~~in this light~~ to obtain comprehensive perspectives on regional rainfall variability. In fact, individual weather systems can exhibit varied spatial characteristics (Habib and Krajewski, 2002; Ciach and Krajewski, 2006; Tokay et al., 2014). In southeastern Austria, including the WEGN area, Schroeer et al. (2018) found much steeper decay in a correlogram function when only extreme summertime convective events are accounted for. Additionally, we found that during the ~~dry~~ cold season, the density of gauges is less of a concern (i.e., longer correlation distance) compared to the ~~wet~~ warm season. However, low values of ~~zero-distance correlation~~ the nugget effect parameter imply that snow ~~measurement~~ measurements during winter time ~~remains~~ remain a challenge, especially at short time scales.

Secondly, we confirm that the 150 gauges of WEGN offer very highly accurate areal precipitation estimates. The overall uncertainty in mean areal rainfall shows ~~there to be a high~~ a clear dependence on the number of gauges and the temporal resolution considered for the estimation. ~~Seeing~~ To reach the same level of accuracy, the average number of gauge has to be increased roughly following a power law as time scale decreases. Given that only two operational meteorological stations exist over the WEGN area, the ~~accuracy of areal rainfall data obtained under normal circumstances could be inadequate for particular purposes~~insufficient gauge density may hamper the use of the station data to construct spatial rainfall fields in the region, especially at sub-daily scales. ~~We also investigated the effect of gauge density on total amount and peak hourly intensity of the daily heavy rainfall events. In the WEGN area (300)~~The accuracy of areal rainfall estimation is also significantly dependent

on the spatial configuration of the network. Assuming that we have a well-distributed gauge network, it is observed that at least 2-5 gauges are required ~~for~~ in the WEGN area (300 km^2) for accurate areal rainfall estimates such that we can obtain reliable rainfall event statistics (e.g., total amount and peak hourly intensity of daily heavy rainfall events) with no significant error. More than ~~5 gauges guarantee a high accuracy of the areal rainfall estimates~~10 gauges guarantee that we can obtain constant results, regardless of number of the gauge. Our findings have implications concerning the use of sparse ~~gauge observational~~ observational gauge data, for instance, in hydrologic modeling or rainfall estimates evaluation (e.g., Syed et al., 2003; Tian et al., 2018).

Lastly, using gridded WEGN data, rainfall extremes are reproduced at multiple spatial scales; approximately from the grid resolution of regional to convective-permitting models (about 11.1 km to 1.1 km in latitudinal direction). ~~The results~~ We show how different rainfall events can be considered extreme depending on the spatial and temporal resolutions. The results also demonstrate that high-resolution gridded data provide more reliable information not only in terms of the magnitude and frequency of extremes, but also in terms of the exact location of the extremes. As a result, ~~the limited spatial scale~~ limited resolution of rainfall data can alter interpretations of rainfall statistics; extreme rainfall events at a location of interest (a $0.01^\circ \times 0.01^\circ$ site in our example) could occur more frequently and more intensely versus the local average. Localized information from high-resolution observation is the key ~~to~~ for developing prevention and protection plans to mitigate potential damages of extreme rainfall in an efficient and adequate way. Our results highlight the need to evaluate uncertainty in extreme statistics derived from the existing datasets for supporting data selection among available rainfall data products.

In conclusion, the WEGN network provides a unique opportunity to empirically assess spatial variability and uncertainty of surface rainfall directly based on gauge data. The network provides long-term records, of more than a decade, which ~~enable obtaining statistically robust results~~permit to exclusively focus on heavy rain events. Nonetheless, as stated in Villarini et al. (2008), there are only a few dense gauge networks on the ~~local~~ catchment scale, so the verification of findings from studies in other regions is challenging. Regional variations, such as topography or rain type, can lead to differences in the degree of rainfall variability and uncertainty (e.g., Buytaert et al., 2006; Prein and Gobiet, 2017). Therefore, some of the general conclusions of this study ~~should only be generalized~~ may only be representative for mid-latitude regions with moderate topography. In addition, more robust interpretation of the rainfall spatial structure beyond the network dimension (> 15 km) needs to be complemented by additional larger-scale gauge data. For instance, Schroeer et al. (2018) used three different scales of networks, including the WEGN, to estimate the underestimation of maximum area precipitation of extreme convective over the range of 1 km to 30 km. It should be noted that WEGN has a high flexibility in terms of providing rainfall data within various spatial scales thanks to both high-resolution and quasi-grid configuration of the gauges. In this context, WEGN will continue providing observational evidence to explore ~~small-to-local~~ local-to-catchment scale rainfall processes over the next years.

Data availability. WegenerNet data products are available at www.wegenernet.org.

Appendix A: ~~Definition of rain-gauge sub-networks~~Heavy rainfall events

~~Figure ??~~ Table A1 shows general information about the selected heavy rainfall events studied in Sect. 4 and Sect. 5. The events are corresponding to $\geq$90th percentile of daily rainfall (06-06 UTC) during the warm season. Peak ratio is given as a ratio of peak hourly rainfall to daily total. Rainfall in the region during the summer months is triggered by the advection of humid air masses from the Adriatic Sea. Heavy rainfall events are closely linked with local thunderstorms (Matulla et al., 2003, see also Sect. 2) . The rain type is not explicitly considered for the event selection.

Appendix B: Definition of rain-gauge sub-networks

Figure A1 shows the selection order of WEGN gauges for defining the low-density sub-networks that were used in Fig. 6 of Sect. 4. Priority consideration was given to the actual location of operational weather stations within the WEGN network; the selected gauges 1 and 2 are located nearest to the member stations of the Austrian weather service (ZAMG) and the gauges 3, 4, and 5 are nearest to the rain gauges operated by the Austrian hydrographic services (AHYD). The gauges ~~afterword~~ afterward were arbitrarily selected, ensuring a spatially uniform distribution. Normalized standard deviation of area-of-influence was used as an index for the uniformity of gauge configuration, which fluctuated between 0.37 and 0.23 with a decreasing trend as the number of the selected gauges increases. The area-of-influence is defined as follows: small grid boxes (approx. $0.01^\circ \times 0.01^\circ$, a total of 406 boxes) were defined over the WEGN network and each box is assigned to the nearest gauges of a given sub-network. Then, with an assumption that the most regular gauge configuration would share the same number of boxes, standard deviation of the area-of-influence of n-gauges is calculated. For instance, for the $five$-gauges sub-network, each gauge is expected to share around 80 boxes under an ideal situation. However, in this study, the five gauges share 71 to 113 boxes each, resulting in the uniformity index of 0.35. Note that this simple method does not consider the degree of centralization.

The uniformity index defined here is also used for Fig. 5 to select well- and badly-distributed n-gauge networks.

Competing interests. The authors declare that they have no conflict of interest.

Acknowledgements. The authors thank ~~Prof~~G. Kirchengast and J. Fuchsberger (University of Graz) for fruitful discussions. The study was ~~fully~~ funded by the Austrian Science Fund (FWF) under research grant W 1256-G15 (Doctoral Programme Climate Change Uncertainties, Thresholds and Coping Strategies). WegenerNet funding is provided by the Austrian Ministry for Science and Research, the University of Graz, the state of Styria (which also included European Union regional development funds), and the city of Graz; detailed information is found at www.wegcenter.at/wegenernet.

References

Bárdossy, A. and Das, T.: Influence of rainfall observation network on model calibration and application, Hydrol. Earth Syst. Sci., 12, 77–89, https://doi.org/10.5194/hess-12-77-2008, 2008.

Berezowski, T., Szcześniak, M., Kardel, I., Michałowski, R., Okruszko, T., Mezghani, A., and Piniewski, M.: CPLFD-GDPT5: High-resolution gridded daily precipitation and temperature data set for two largest Polish river basins, Earth Syst. Sci. Data, 8, 127–139, https://doi.org/10.5194/essd-8-127-2016, 2016.

Buytaert, W., Celleri, R., Willems, P., Biévre, B. D., and Wyseure, G.: Spatial and temporal rainfall variability in mountainous areas: A case study from the south Ecuadorian Andes, J. Hydrol., 329, 413–421, https://doi.org/10.1016/j.jhydrol.2006.02.031, 2006.

Chaudhary, S., Dhanya, C., and Vinnarasi, R.: Dry and wet spell variability during monsoon in gauge-based gridded daily precipitation datasets over India, J. Hydrol, 546, 204–218, https://doi.org/10.1016/j.jhydrol.2017.01.023, 2017.

Ciach, G. J. and Krajewski, W. F.: On the estimation of radar rainfall error variance, Adv. Water Resour., 22, 585–595, https://doi.org/10.1016/S0309-1708(98)00043-8, 1999.

Ciach, G. J. and Krajewski, W. F.: Analysis and modeling of spatial correlation structure in small-scale rainfall in Central Oklahoma, Adv. Water Resour., 29, 1450–1463, https://doi.org/10.1016/j.advwatres.2005.11.003, 2006.

Contractor, S., Alexander, L. V., Donat, M. G., and Herold, N.: How well do gridded datasets of observed daily precipitation compare over Australia?, Adv. Meteorol., 2015, 1–15, https://doi.org/10.1155/2015/325718, 2015.

Dai, A., Lin, X., and Hsu, K.-L.: The frequency, intensity, and diurnal cycle of precipitation in surface and satellite observations over low- and mid-latitudes, Clim. Dyn., 29, 727–744, https://doi.org/10.1007/s00382-007-0260-y, 2007.

Dhib, S., Mannaerts, C. M., Bargaoui, Z., Retsios, V., and Maathuis, B. H.: Evaluating the MSG satellite Multi-Sensor Precipitation Estimate for extreme rainfall monitoring over northern Tunisia, Weather Clim Extrem, 16, 14–22, https://doi.org/10.1016/j.wace.2017.03.002, 2017.

Eggert, B., Berg, P., Haerter, J. O., Jacob, D., and Moseley, C.: Temporal and spatial scaling impacts on extreme precipitation, Atmos. Chem. Phys., 15, 5957–5971, https://doi.org/10.5194/acp-15-5957-2015, 2015.

Gebremichael, M. and Krajewski, W. F.: Assessment of the statistical characterization of small-scale rainfall variability from radar: analysis of TRMM ground validation datasets, J. Appl. Meteorol. Clim., 43, 1180–1199, 2004.

Girons Lopez, M., Wennerström, H., Nordén, L.-Å., and Seibert, J.: Location and density of rain gauges for the estimation of spatial varying precipitation, Geogr. Ann.: Ser. A, Phys. Geogr., 97, 167–179, https://doi.org/10.1111/geoa.12094, 2015.

Habib, E. and Krajewski, W. F.: Uncertainty analysis of the TRMM ground-validation radar-rainfall products: Application to the TEFLUN-B field campaign, J. Appl. Meteorol. Clim., 41, 558–572, https://doi.org/10.1175/1520-0450(2002)041<0558:UAOTTG>2.0.CO;2, 2002.

Habib, E., Krajewski, W. F., and Ciach, G. J.: Estimation of rainfall interstation correlation, J. Hydrometeorol., 2, 621–629, https://doi.org/10.1175/1525-7541(2001)002<0621:EORIC>2.0.CO;2, 2001.

Hofstra, N., New, M., and McSweeney, C.: The influence of interpolation and station network density on the distributions and trends of climate variables in gridded daily data, Clim. Dyn., 35, 841–858, https://doi.org/10.1007/s00382-009-0698-1, 2010.

Hou, A. Y., Kakar, R. K., Neeck, S., Azarbarzin, A. A., Kummerow, C. D., Kojima, M., Oki, R., Nakamura, K., and Iguchi, T.: The Global Precipitation Measurement mission, Bull Am Meteorol Soc., 95, 701–722, https://doi.org/10.1175/BAMS-D-13-00164.1, 2014.

Huff, F. A. and Shipp, W. L.: Spatial correlations of storm, monthly and seasonal precipitation, J. Appl. Meteorol. Climatol, 8, 542–550, https://doi.org/10.1175/1520-0450(1969)008<0542:SCOSMA>2.0.CO;2, 1969.

Jaffrain, J. and Berne, A.: Quantification of the small-scale spatial structure of the raindrop size distribution from a network of disdrometers, J. Appl. Meteorol. Clim., 51, 941–953, https://doi.org/10.1175/JAMC-D-11-0136.1, 2012.

Kann, A., Meirold-Mautner, I., Schmid, F., Kirchengast, G., Fuchsberger, J., Meyer, V., T'uchler, L., and Bica, B.: Evaluation of high-resolution precipitation analyses using a dense station network, 19, 1547–1559, https://doi.org/10.5194/hess-19-1547-2015, 2015.

Keller, V. D. J., Tanguy, M., Prosdocimi, I., Terry, J. A., Hitt, O., Cole, S. J., Fry, M., Morris, D. G., and Dixon, H.: CEH-GEAR: 1 km resolution daily and monthly areal rainfall estimates for the UK for hydrological and other applications, Earth Syst. Sci. Data, 7, 143–155, https://doi.org/10.5194/essd-7-143-2015, 2015.

Kirchengast, G., Kabas, T., Leuprecht, A., Bichler, C., and Truhetz, H.: WegenerNet: A pioneering high-resolution network for monitoring weather and climate, Bull. Amer. Meteor. Soc., 95, 227–242, https://doi.org/10.1175/BAMS-D-11-00161.1, 2014.

Lockhoff, M., Zolina, O., Simmer, C., and Schulz, J.: Evaluation of satellite-retrieved extreme precipitation over Europe using gauge observations, J. Clim, 27, 607–623, https://doi.org/10.1175/JCLI-D-13-00194.1, 2014.

Ly, S., Charles, C., and Degré, A.: Geostatistical interpolation of daily rainfall at catchment scale: The use of several variogram models in the Ourthe and Ambleve catchments, Belgium, Hydrol. Earth Syst. Sci., 15, 2259–2274, https://doi.org/10.5194/hess-15-2259-2011, 2011.

Marra, F., Destro, E., Nikolopoulos, E. I., Zoccatelli, D., Creutin, J. D., Guzzetti, F., and Borga, M.: Impact of rainfall spatial aggregation on the identification of debris flow occurrence thresholds, Hydrol. Earth Syst. Sci., 21, 4525–4532, https://doi.org/10.5194/hess-21-4525-2017, 2017.

Matulla, C., Penlap, E. K., Haas, P., and Formayer, H.: Comparative analysis of spatial and seasonal variability: Austrian precipitation during the 20th century, Int. J. Climatol., 23, 1577–1588, https://doi.org/10.1002/joc.960, 2003.

O, S., Foelsche, U., Kirchengast, G., and Fuchsberger, J.: Validation and correction of rainfall data from the WegenerNet high density network in southeast Austria, J. Hydrol., 556, 1110–1122, https://doi.org/10.1016/j.jhydrol.2016.11.049, 2018a.

O, S., Foelsche, U., Kirchengast, G., Fuchsberger, J., Tan, J., and Petersen, W. A.: Evaluation of GPM IMERG Early, Late, and Final rainfall estimates using WegenerNet gauge data in southeastern Austria, Hydrol. Earth Syst. Sci., 21, 6559–6572, https://doi.org/10.5194/hess-21-6559-2017, 2018b.

Peleg, N., Ben-Asher, M., and Morin, E.: Radar subpixel-scale rainfall variability and uncertainty: Lessons learned from observations of a dense rain-gauge network, Hydrol. Earth Syst. Sci., 17, 2195–2208, https://doi.org/10.5194/hess-17-2195-2013, 2013.

Prein, A. F. and Gobiet, A.: Impacts of uncertainties in European gridded precipitation observations on regional climate analysis: Uncertainty in European Precipitation, Int. J. Climatol., 37, 305–327, https://doi.org/10.1002/joc.4706, 2017.

Schroeer, K., Kirchengast, G., and O, S.: Strong dependence of extreme convective precipitation intensities on gauge network density, Geophys. Res. Lett., https://doi.org/10.1029/2018GL077994, accepted, 2018.

Sillmann, J., Thorarinsdottir, T., Keenlyside, N., Schaller, N., Alexander, L. V., Hegerl, G., Seneviratne, S. I., Vautard, R., Zhang, X., and Zwiers, F. W.: Understanding, modeling and predicting weather and climate extremes: Challenges and opportunities, Weather. Clim. Soc., 18, 65–74, https://doi.org/10.1016/j.wace.2017.10.003, 2017.

Steiner, M., Smith, J. A., Burges, S. J., Alonso, C. V., and Darden, R. W.: Effect of bias adjustment and rain gauge data quality control on radar rainfall estimation, Water Resour. Res., 35, 2487–2503, https://doi.org/10.1029/1999WR900142, 1999.

Svensson, C. and Jones, D.: Review of methods for deriving areal reduction factors: Review of ARF methods, J. Flood Risk Manag., 3, 232–245, https://doi.org/10.1111/j.1753-318X.2010.01075.x, 2010.

Svoboda, V., Máca, P., Hanel, M., and Pech, P.: Spatial correlation structure of monthly rainfall at a mesoscale region of north-eastern Bohemia, Theor. Appl. Climatol, 121, 359–375, https://doi.org/10.1007/s00704-014-1241-9, 2015.

Syed, K. H., Goodrich, D. C., Myers, D. E., and Sorooshian, S.: Spatial characteristics of thunderstorm rainfall fields and their relation to runoff, J. Hydrol., 271, 1–21, https://doi.org/10.1016/S0022-1694(02)00311-6, 2003.

Tan, J., Petersen, W. A., Kirchengast, G., Goodrich, D. C., and Wolff, D. B.: Evaluation of Gobal Precipitation Measurement rainfall estimates against three dense gauge networks, 19, 517–532, https://doi.org/10.1175/JHM-D-17-0174.1, 2018.

Tian, F., Hou, S., Yang, L., Hu, H., and Hou, A.: How does the evaluation of the GPM IMERG rainfall product depend on gauge density and rainfall intensity?, J. Hydrometeorol., 19, 339–349, https://doi.org/10.1175/JHM-D-17-0161.1, 2018.

Tokay, A., Roche, R. J., and Bashor, P. G.: An experimental study of spatial variability of rainfall, J. Hydrometeorol., 15, 801–812, https://doi.org/10.1175/JHM-D-13-031.1, 2014.

Tozer, C. R., Kiem, A. S., and Verdon-Kidd, D. C.: On the uncertainties associated with using gridded rainfall data as a proxy for observed, Hydrol. Earth Syst. Sci., 16, 1481–1499, https://doi.org/10.5194/hess-16-1481-2012, 2012.

Villarini, G., Mandapaka, P. V., Krajewski, W. F., and Moore, R. J.: Rainfall and sampling uncertainties: A rain gauge perspective, J. Geophys. Res., 113, https://doi.org/10.1029/2007JD009214, 2008.

Wood, S. J., Jones, D. A., and Moore, R. J.: Accuracy of rainfall measurement for scales of hydrological interest, Hydrol. Earth Syst. Sci., 4, 531–543, https://doi.org/10.5194/hess-4-531-2000, 2000.

Xu, H., Xu, C.-Y., Chen, H., Zhang, Z., and Li, L.: Assessing the influence of rain gauge density and distribution on hydrological model performance in a humid region of China, J. Hydrol., 505, 1–12, https://doi.org/10.1016/j.jhydrol.2013.09.004, 2013.

Yatagai, A., Kamiguchi, K., Arakawa, O., Hamada, A., Yasutomi, N., and Kitoh, A.: APHRODITE: Constructing a long-term daily gridded precipitation dataset for Asia based on a dense network of rain gauges, Bull Am Meteorol Soc., 93, 1401–1415, https://doi.org/10.1175/BAMS-D-11-00122.1, 2012.

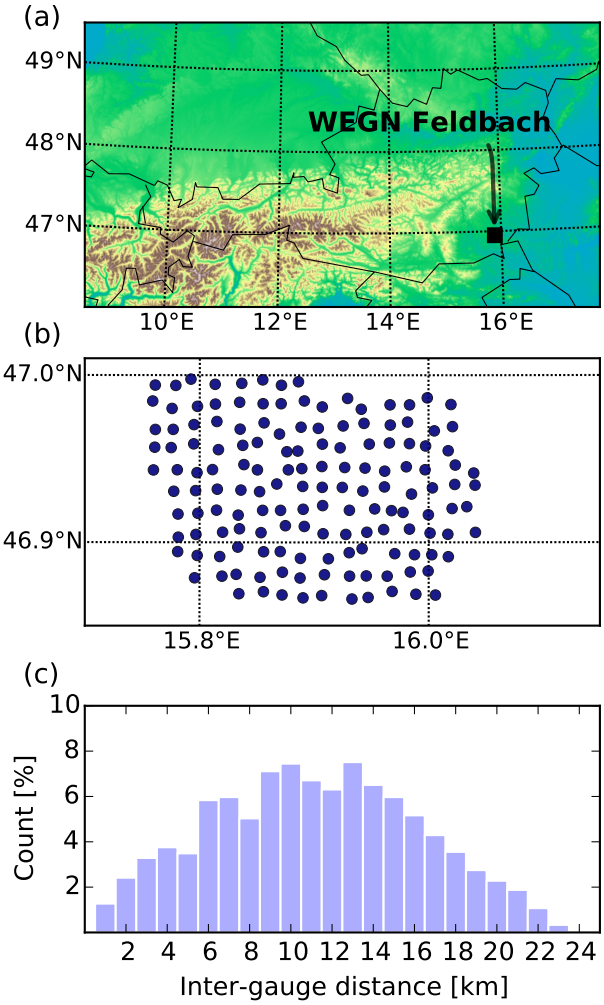

Figure 1. (a) WegenerNet Feldbach region (WEGN) network in southeastern Austria, (b) location of 150 tipping-bucket rain gauges, and (c) inter-gauge distances, rounded to the nearest 1-km bins.

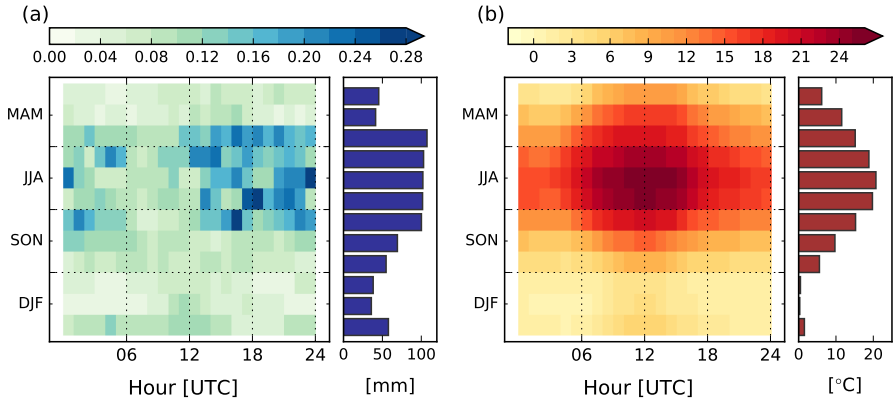

Figure 2. Diurnal cycles of (a) rainfall and (b) temperature derived from WEGN observational data.

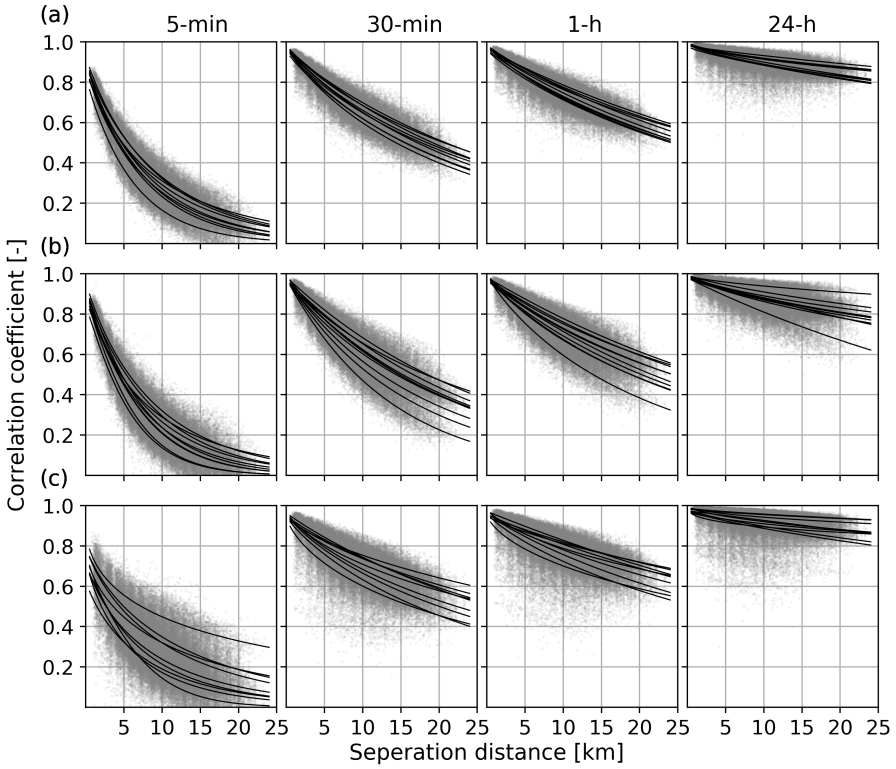

Figure 3. Spatial correlation of rainfall among rain gauges for (a) all-months, (b) ~~wet~~ warm season, and (c) ~~dry~~ cold season. Four selected accumulation times are shown. Each solid line represents a fitted exponential function for each year.

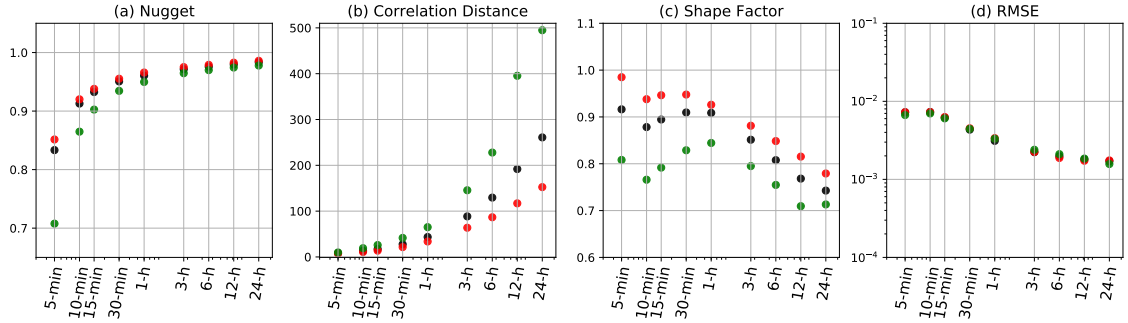

Figure 4. Dependence of (a) nugget effect, (b) correlation distance, and (c) shape factor of the fitted exponential functions on timescale. (d) shows RMSE of fitted correlation values compared to observed values (red: ~~wet~~ warm season, green: ~~dry~~ cold season, black: all-months).

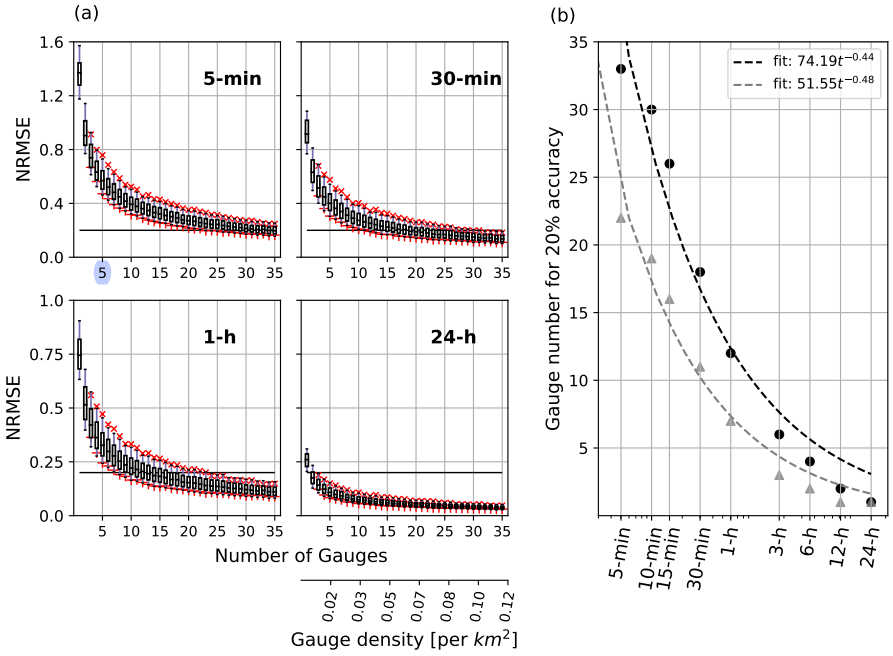

Figure 5. Dependence of the accuracy of areal rainfall estimates on the number of gauges during heavy rainfall. Normalised RMSEs (NRMSEs) of 1,000 different gauge combinations are used to assess the accuracy for each n-gauge network. (a) Four selected time accumulation are shown. Box plots display the median, 25th and 75th percentiles of NRMSE distribution, and whiskers extend to the 10th and 90th percentiles. Red crosses and Xs show the median NRMSE for good and bad gauge configurations; 100 cases are selected, respectively, for each of the 1,000 combinations. (b) The average and minimum number of gauges (black and gray, respectively) required to obtain areal rainfall estimates with an ~~normalized RMSE~~ NRMSE < 20%.

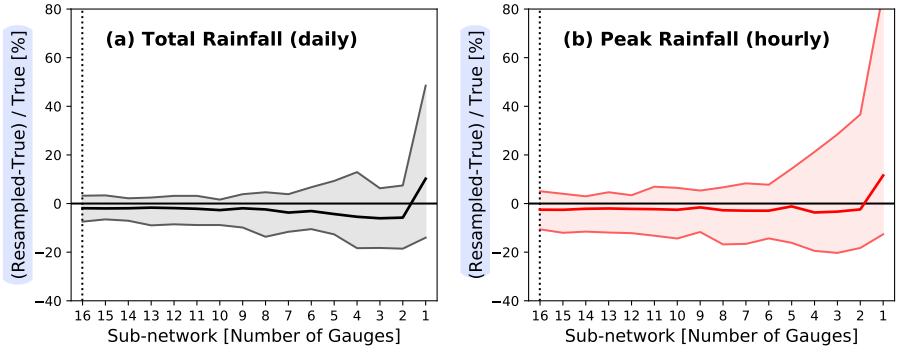

Figure 6. Dependence of the accuracy of (a) daily rainfall and (b) hourly peak intensity on the number of gauges. 71 heavy rain events are considered. The y axis displays the ~~ratio of~~ relative difference between resampled ~~rainfall to~~ and true rainfall. Resampled rainfall is calculated from n-gauge sub-networks, while true rainfall is calculated using the full density WEGN network. The thick lines show the median and the shaded areas show the 10th to 90th percentile spread.

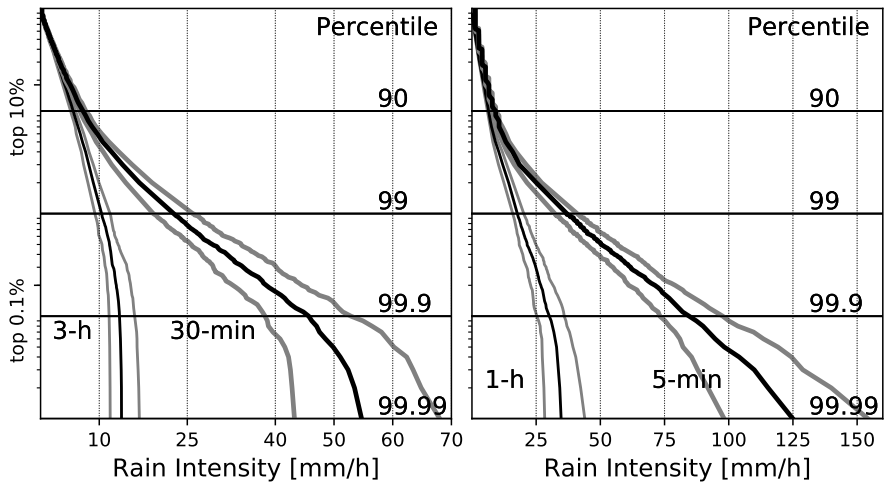

Figure 7. Distribution of gauge-level rainfall intensities corresponding to given percentile thresholds during heavy rainfall events. Four time scales are selected. Black lines show median values, gray lines show a 10th-90th percentile range among the gauges at a given threshold bin.

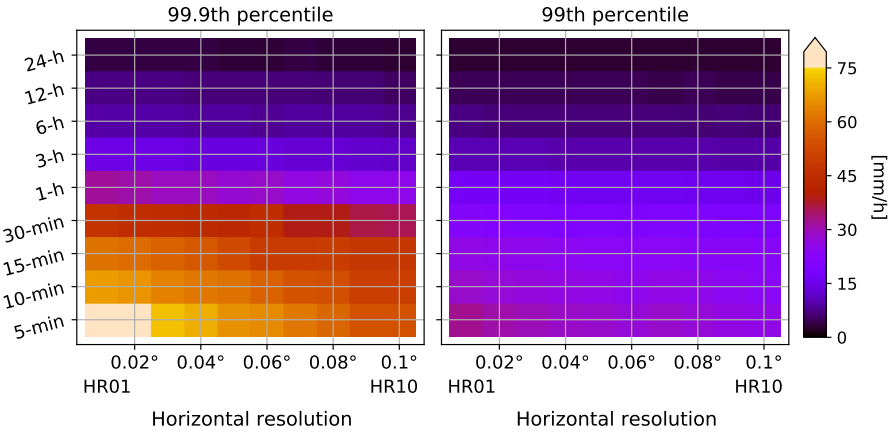

Figure 8. 99.9th and 99th percentiles of rainfall intensities derived from gridded rainfall fields with different spatial and temporal scales.

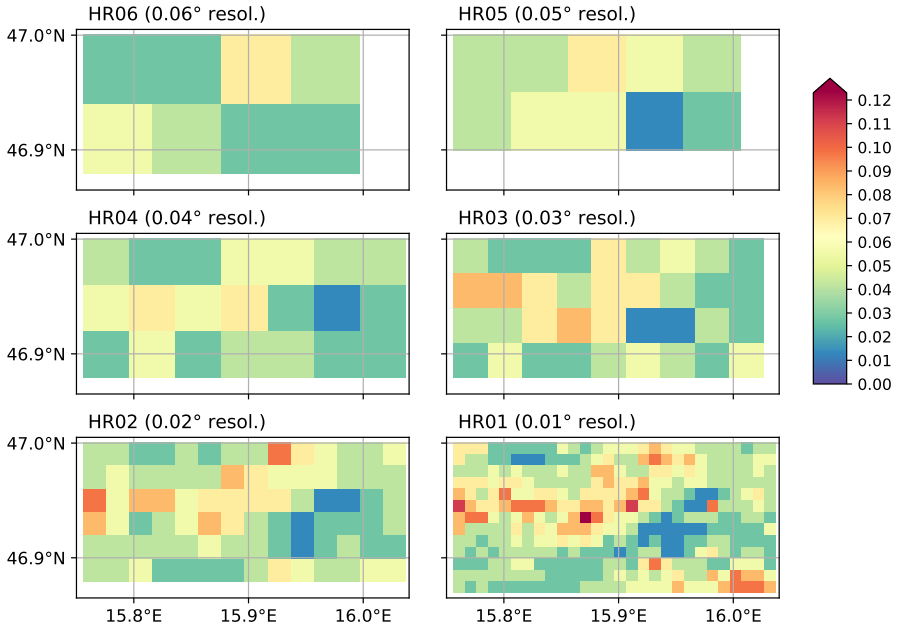

Figure 9. Occurrence of extreme events ($\geq$ 95th percentile of rainfall intensity during heavy rainfall events at HR01) at different horizontal grid spacing.

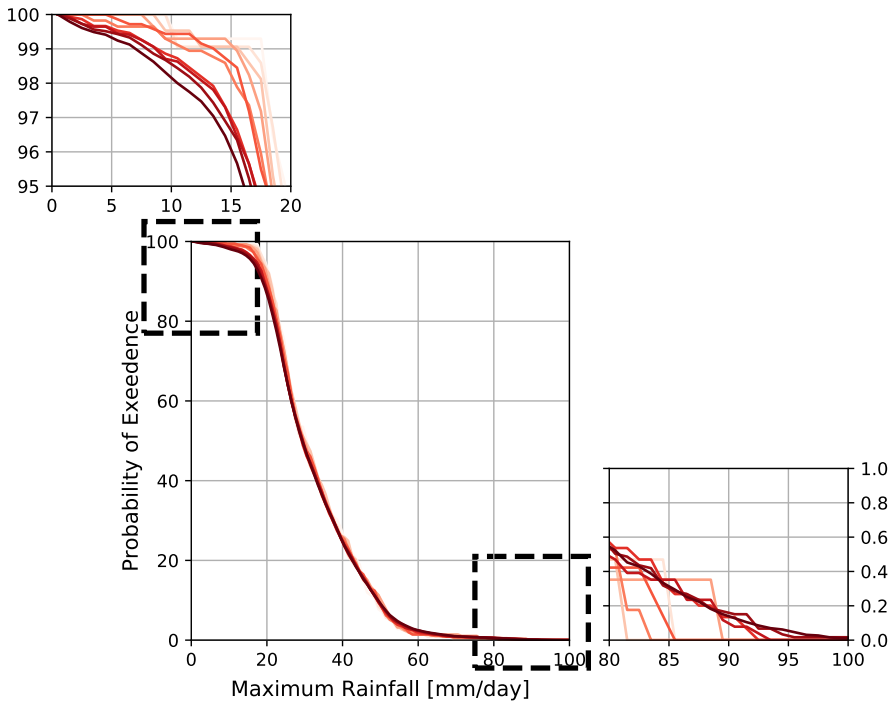

Figure 10. Probability of occurrence of heavy rainfall for different horizontal resolutions. Darker red represents higher horizontal resolution (from 0.1° to 0.01°).

Table A1. Information of selected heavy rainfall events

	Min	Median	Max
Total rainfall ($\mathrm{mm\,d^{-1}}$)	19.8	28.1	64.1
Peak hourly rainfall ($\mathrm{mm\,h^{-1}}$)	2.6	8.6	26.2
Peak ratio	7.8	25.4	91.0
Duration (h)	2.0	9.5	22.5

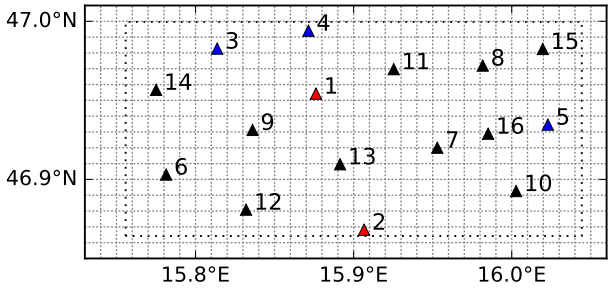

Figure A1. Selected WEGN gauges for Fig. 6. The gauges nearest to operational weather stations of the ZAMG and AHYD are in red and blue, respectively.